Article

Developmental Cell

A Cranial Mesoderm Origin for Esophagus Striated Muscles

Graphical Abstract

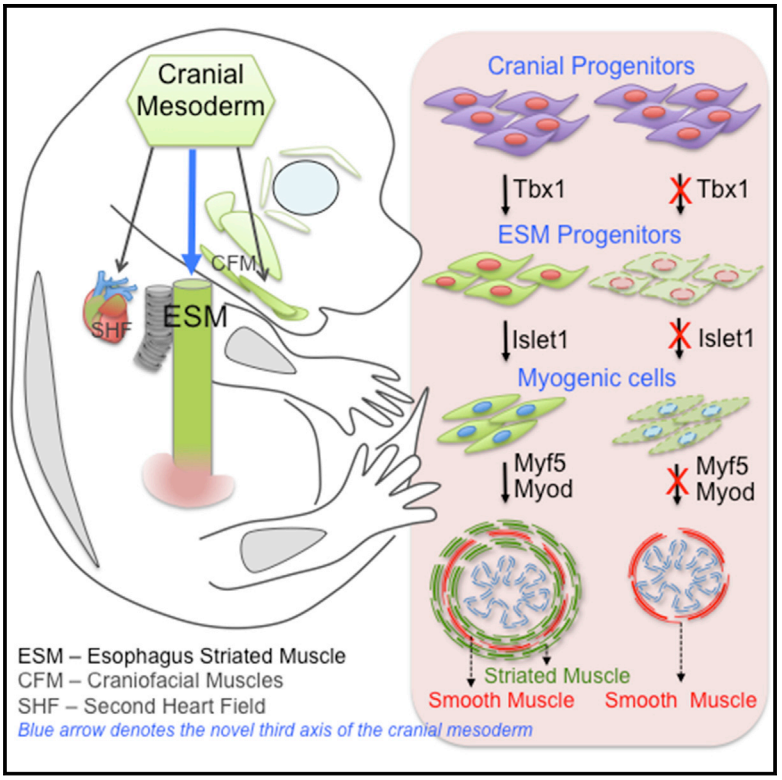

Authors

Swetha Gopalakrishnan, Glenda Comai, Ramkumar Sambasivan, Alexandre Francou, Robert G. Kelly, Shahragim Tajbakhsh

Correspondence

shahragim.tajbakhsh@pasteur.fr

In Brief

Gopalakrishnan et al. show that esophagus striated muscles are cranial, not somitic, in origin and form a third derivative of the cranial mesoderm that also gives rise to head muscles and second heart field derived parts of the heart.

Highlights

- Esophagus striated muscles (ESMs) originate from cranial, not somitic, mesoderm
- *Tbx1* mutant mice are devoid of ESMs
- *Tbx1*-dependent *Isl1* progenitors seed and pattern ESMs in an anterior-posterior direction
- ESMs uniquely adopt a fetal myogenic program using smooth muscle as a scaffold

Gopalakrishnan et al., 2015, Developmental Cell *34*, 694–704
September 28, 2015
http://dx.doi.org/10.1016/j.devcel.2015.07.003

CellPress

Developmental Cell
Article

A Cranial Mesoderm Origin for Esophagus Striated Muscles

Swetha Gopalakrishnan,[1] Glenda Comai,[1] Ramkumar Sambasivan,[2] Alexandre Francou,[3] Robert G. Kelly,[3] and Shahragim Tajbakhsh[1,*]

[1]Department of Developmental & Stem Cell Biology, Institut Pasteur, Stem Cells & Development, CNRS URA 2578, 25 Rue du Dr. Roux, 75015 Paris, France

[2]Institute for Stem Cell Biology and Regenerative Medicine, GKVK P.O., Bellary Road, Bangalore 560065, India

[3]Aix Marseille Université, CNRS, IBDM UMR 7288, 13288 Marseille, France

*Correspondence: shahragim.tajbakhsh@pasteur.fr

http://dx.doi.org/10.1016/j.devcel.2015.07.003

SUMMARY

The esophagus links the oral cavity to the stomach and facilitates the transfer of bolus. Using genetic tracing and mouse mutants, we demonstrate that esophagus striated muscles (ESMs) are not derived from somites but are of cranial origin. *Tbx1* and *Isl1* act as key regulators of ESMs, which we now identify as a third derivative of cardiopharyngeal mesoderm that contributes to second heart field derivatives and head muscles. *Isl1*-derived ESM progenitors colonize the mouse esophagus in an anterior-posterior direction but are absent in the developing chick esophagus, thus providing evolutionary insight into the lack of ESMs in avians. Strikingly, different from other myogenic regions, in which embryonic myogenesis establishes a scaffold for fetal fiber formation, ESMs are established directly by fetal myofibers. We propose that ESM progenitors use smooth muscle as a scaffold, thereby bypassing the embryonic program. These findings have important implications in understanding esophageal dysfunctions, including dysphagia, and congenital disorders, such as DiGeorge syndrome.

INTRODUCTION

The act of swallowing propels bolus through the esophagus to the stomach by triggering sequential radial waves of striated and smooth muscle contractions called peristalsis, which is largely under the autonomic control of the central and peripheral mechanisms (Yazaki and Sifrim, 2012). Interestingly, the proportion of striated muscles that compose the esophagus wall varies extensively across vertebrate species, being absent in avians and reptiles and present in part of, or in the entire, esophagus, in ruminants and rodents (Shiina et al., 2005). In humans, the esophagus wall is composed of striated muscles in the upper part, whereas the lower portion is comprised only of smooth muscles. The developmental and evolutionary origin of striated muscles in the esophagus remains unclear, despite the importance of esophagus striated muscles (ESMs) in a spectrum of human esophageal dysfunctions, including idiopathic myopathy, motility disorders, achalasia, and dysphagia (Kilic et al., 2003; Rózsai et al., 2009; Sheehan, 2008).

In most vertebrate embryos, the muscularis externa (external muscle layer) of the esophagus develops as an outer longitudinal and inner circular layer of smooth muscle, which is subsequently replaced by striated muscles as development proceeds. ESMs were proposed to arise through a unique transdifferentiation of smooth muscle fibers (Patapoutian et al., 1995). However, ensuing lineage-tracing studies provided evidence that the striated muscles of the esophagus originate from precursors distinct from that of the smooth muscle (Rishniw et al., 2003; Zhao and Dhoot, 2000). In vertebrates, the bHLH myogenic regulatory factors (MRFs) Myf5, Mrf4, Myod, and Myogenin play crucial roles in governing striated muscle cell fate and differentiation (Kassar-Duchossoy et al., 2004; Rudnicki et al., 1993). All body muscles and part of the tongue musculature are established from founder stem cells located in transient structures called somites, and they are under the regulation of the paired/homeobox transcription factors *Pax3* and *Pax7* (Kassar-Duchossoy et al., 2005; Relaix et al., 2005). In contrast, the founder stem cells of cranial muscles do not express *Pax3* (Relaix et al., 2004), as they are regulated by a distinct genetic program (Sambasivan et al., 2009; Tajbakhsh et al., 1997).

As chordates evolved from filter feeders to active predators, the newly elaborated head and mastication muscles developed from the cranial mesoderm, which is regulated by a distinct set of upstream genes, particularly *Tbx1*, *Pitx2*, and *Islet1* (*Isl1*) (Diogo et al., 2015; Grifone and Kelly, 2007; Harel et al., 2009). Apart from the cucullaris-derived trapezius muscle in the neck that was reported to originate from progenitors in the occipital lateral plate mesoderm, the muscles located between the head and trunk are poorly characterized (Diogo et al., 2015; Theis et al., 2010). Recently, the non-somite derived neck muscles were reported to share a common origin with the myocardium (Lescroart et al., 2015). However, striated muscles of the esophagus are generally proposed to arise from *Pax3*+ somitic founder myogenic cells in mouse and fish (Minchin et al., 2013; Romer et al., 2013). Here, we demonstrate that esophagus striated muscles are not somite derived in mouse, but that they follow a cranial myogenic program. Using extensive genetic lineage and mutant analysis in mouse, we demonstrate that ESMs are a newly described third derivative of the pharyngeal mesoderm in addition to head muscles and derivatives of the second heart field, with unique properties that have not been reported for other striated muscles investigated to date.

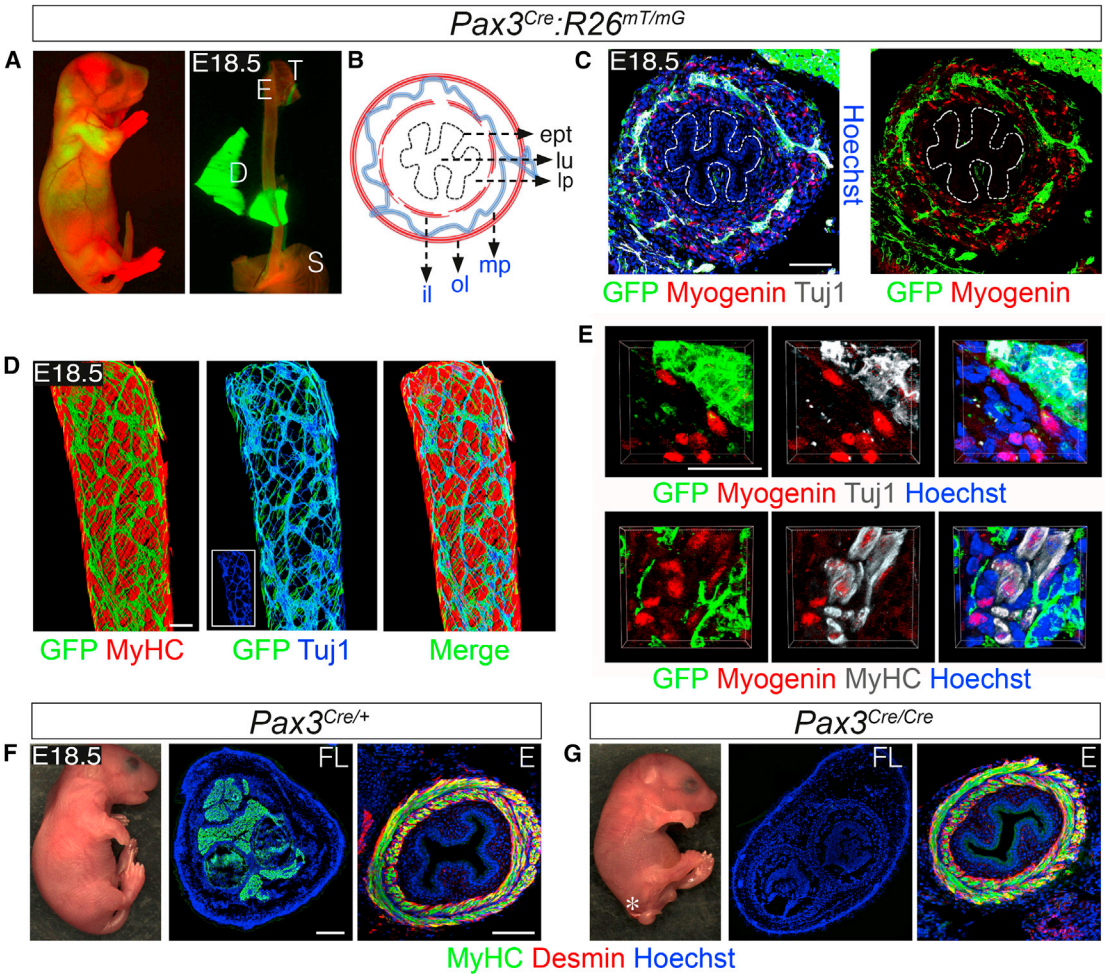

Figure 1. *Pax3*-Derived Somitic Progenitors Do Not Contribute to Esophagus Striated Muscles

(A) A whole-mount macroscopic image of E18.5 *Pax3*$^{Cre/+}$:*R26*$^{mT-mG/+}$ fetus (A, left) and esophagus (A, right; E, esophagus; T, trachea; D, diaphragm; S, stomach; n = 3).

(B) A scheme depicting the two distinct striated muscle layers of the esophagus (il, inner layer; ol, outer layer), the enteric neurons (mp, myenteric plexus) interspersed between these layers, the epithelia (ept), lamina propria (lp), and esophageal lumen (lu).

(C) Immunostaining on transverse sections of anterior esophagus of E18.5 *Pax3*$^{Cre/+}$:*R26* $^{mT-mG/+}$ fetus for GFP+ (green, *Pax3*-lineage derived membrane GFP+ cells), myogenic (red, Myogenin), and neuronal (gray, βIII-tubulin, Tuj1) markers. The dotted line demarcates the esophagus lumen (n = 3). Note major overlap between Tuj1 and membrane GFP+ *Pax3*-lineage-derived cells.

(D) Whole-mount immunofluorescence, followed by 3D reconstruction of E18.5 *Pax3*$^{Cre/+}$:*R26*$^{mT-mG/+}$ esophagus (anterior end) for GFP (green, *Pax3*-lineage derived membrane GFP+ cells) and striated muscle markers (red, MyHC; blue, neuronal Tuj1; n = 3).

(E) High-magnification views of the 3D reconstructions of z stacks images in (C). Note that GFP+ *Pax3*-lineage-derived cells are in close proximity to myogenic (Myogenin+) cells; however, staining overlaps only with the neuronal marker Tuj1, and not with the differentiated muscle marker MyHC.

(F) E18.5 *Pax3*$^{Cre/+}$ fetus with corresponding anterior esophageal section stained for MyHC (green) and Desmin (red), and limb stained for MyHC (n = 3). FL, forelimb; E, esophagus.

(G) Same as in (F) for *Pax3*$^{Cre/Cre}$ mutant (spina bifida*).

Scale bars represent 50 μm (C, D, F, and G [E, esophagus]), 10 μm (E), and 100 μm (F and G [FL]).

See also Figure S1.

RESULTS

Pax3-Derived Somitic Progenitors Do Not Contribute to Mouse ESMs

To investigate the embryological origin of ESM progenitors, we marked somite-derived myogenic cells genetically by crossing *Pax3*^{Cre} mice (Engleka et al., 2005) to a ubiquitous double-fluorescent *Cre* reporter line, *Rosa*$^{mTomato/mGFP}$ (*R26*$^{mT/mG}$;(Muzumdar et al., 2007), in which Cre-mediated recombination labels all the *Pax3*-derived cells with membrane-targeted GFP (mGFP+). If striated muscles of the esophagus were derived from somitic muscle progenitors, we would expect mGFP+ ESM in these mice. Surprisingly, whole-mount macroscopic analysis of E18.5 esophagus showed no contribution of *Pax3*-derived mGFP cells to ESMs, whereas diaphragm and trunk muscles were fully labeled as expected (Figure 1A). Immunostainings of E18.5

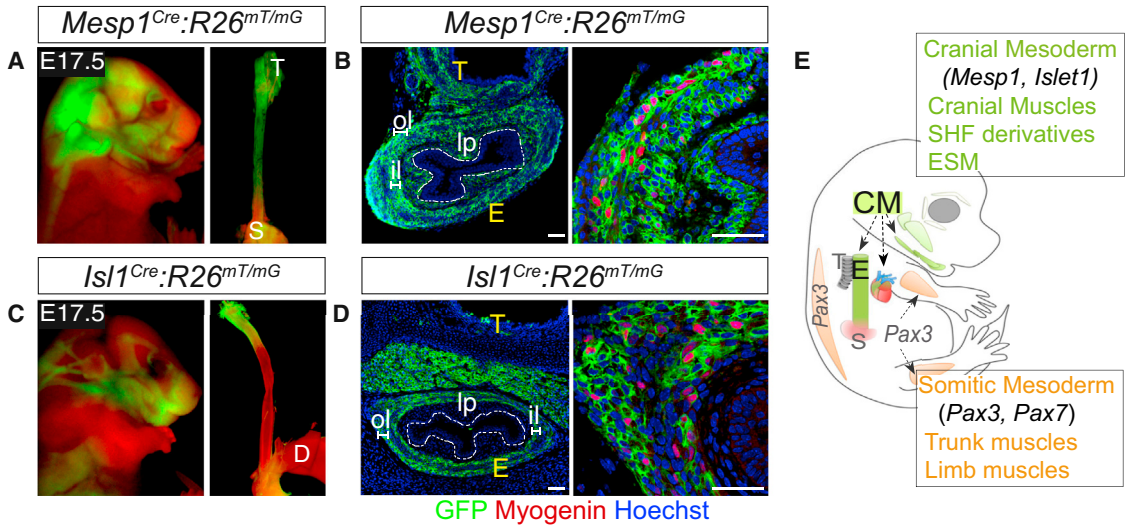

Figure 2. Progenitors of Esophagus Striated Muscles Are Cranial Mesoderm Derived

(A) Whole-mount macroscopic image of E17.5 *Mesp1*$^{Cre/+}$*:R26*$^{mT\text{-}mG/+}$ fetus and dissected esophagus.

(B) Immunofluorescence staining on transverse sections of anterior segment of E17.5 *Mesp1*$^{Cre/+}$*:R26*$^{mT\text{-}mG/+}$ esophagus for GFP (green, *Mesp1*-lineage derived membrane GFP+ cells) and myogenic marker Myogenin (red) (right; n = 2). il, inner layer; ol, outer layer; lp, lamina propria; T, trachea; E, esophagus; D, diaphragm; S, stomach.

(C) Same as in (A) for E17.5 *Isl1*$^{Cre/+}$*:R26*$^{mT\text{-}mG/+}$ embryos (n = 3).

(D) Same as in (B) for E17.5 *Isl1*$^{Cre/+}$*:R26*$^{mT\text{-}mG/+}$ embryos (n = 3).

(E) A scheme summarizing the cranial mesoderm origin of esophageal striated muscles (ESMs). SHF, second heart field.

Scale bars represent 200 μm (B and D, left), 20 μm (B and D, right).

See also Figure S2.

Pax3^{Cre}*:R26*$^{mT/mG}$ esophagus (see Figure 1B) showed no co-localization of mGFP^{+} cells with the myogenic markers tested (Myogenin, MyHC; Figures 1C, 1D, and S1A; data not shown). Instead, we observed abundant *Pax3*-derived mGFP+ cells interspersed in between the outer and inner esophageal muscle layers, in neuron-specific class III β-tubulin (Tuj1)-expressing cells (Figure 1C) that form the Myenteric plexus, as well as the innervation spanning the entire length of the esophagus (Figure 1D). This observation is in accordance with the report that *Pax3*-expressing neural crest cells contribute to the enteric ganglia of the gut (Lang et al., 2000). In the esophagus, *Pax3*-derived mGFP+ cells also contributed to vascular endothelial cells, but not to the smooth muscle cells (data not shown). Thus, our results show that the *Pax3* lineage does not contribute to striated muscles of the esophagus, but largely contributes to its innervation.

However, these results contradict a previous report that ESMs are derived from *Pax3*+ migratory somitic progenitors (Minchin et al., 2013). Careful analysis of the myogenic cells in the *Pax3*$^{Cre/+}$*: R26*$^{mT/mG}$ E18.5 embryos (992 cells counted; n = 3) showed no co-localization of myogenic markers with mGFP+ cells as would have been expected if the myogenic cells were *Pax3* derived (Figure 1E). Immunohistochemistry, followed by high-resolution confocal 3D analysis, revealed that the few myogenic cells that appeared to be in close proximity to GFP+ cells and might be scored as co-expressing (Figures S1A and S1B) were in fact positioned in a different optical plane and were not mGFP+ (Figure S1C). In contrast, the myogenic cells from *Pax3*-derived neck muscles were all mGFP+ (Figure S1D, yellow arrowheads), suggesting the absence of even a minor contribution of *Pax3*-derived cells to ESMs. Using the same Cre-Reporter combination as the previous study reporting Pax3-derived somite progenitors in the esophagus (Minchin et al., 2013), our analysis of E18.5 *Pax3*$^{Cre/+}$*: Z/AP* fetuses confirmed our observations that *Pax3*-derived cells did not contribute to the ESMs (Figure S1E).

To verify our findings, we employed a sensitive *Pax7* lineage-specific reporter *Pax7*$^{nGFP\text{-}stop/nlacZ}$ (hereafter, *Pax7*^{GPL}; (Sambasivan et al., 2013). We found that in the esophagus of E18.5 *Pax3*$^{Cre:}$*:Pax7*^{GPL} fetuses, there was no contribution of *Pax3*-derived cells to ESMs whereas all other trunk muscles were robustly labeled as expected (nlacZ+; Figures S1F and S1G). Finally, in accordance with the genetic lineage tracing results, analysis of E18.5 *Pax3*$^{Cre/+}$ (control) and *Pax3*$^{Cre/Cre}$ (mutant) embryos showed that ESMs were unaffected in the *Pax3* mutants (Figures 1F, 1G, and S1H), whereas somite-derived limb muscles were entirely lacking as expected (Daston et al., 1996). These results conclusively demonstrate that *Pax3*-derived migratory somitic progenitors are not required for ESM development and point to a non-somitic origin of ESMs.

ESMs Are Derived from Cardiopharyngeal Mesoderm

An early-stage marker of cranial mesodermal (CM) cells is Mesoderm progenitor 1 (*Mesp1*) (Harel et al., 2009; Saga et al., 2000). Interestingly, lineage mapping with *Mesp1*^{Cre}*:R26*$^{mT/mG}$ showed robust expression of mGFP in all cranial mesoderm-derived structures, as well as in the esophagus (Figure 2A). Immunostaining of the esophageal sections with myogenic markers (Myogenin and Pax7) showed that ESM is derived from *Mesp1*-expressing cells (Figures 2B and S2A). In addition to the ESMs,

Mesp1-derived mGFP also marked the connective tissue, the lamina propria (lp), but not the smooth muscles of the esophagus (Figure S2B). While *Mesp1* marks CM widely, the *Isl1*-expressing subpopulation of CM constituting the cardiopharyngeal mesoderm (CpM) is known to contribute to pharyngeal arch-derived muscles, in addition to parts of the heart derived from the second heart field (Nathan et al., 2008). Analysis of E17.5 $Isl1^{Cre}$*: R26*$^{mT/mG}$ embryos showed contribution of *Isl1*-derived CpM cells to ESMs (Myogenin, MyHC, and Pax7), but not to the lamina propria or smooth muscle layer (Figures 2C, 2D, and S2C–S2F), thus providing further evidence that ESMs are a third derivative of the CpM (Figure 2E).

Isl1-Derived Myogenic Progenitors Colonize and Pattern ESMs in an A-P Direction

Having established that ESMs are the derivatives of *Isl1*-expressing cranial CpM, we next analyzed the spatiotemporal patterning of ESM progenitors in the esophagus. First, to investigate the developmental timing of the emergence of myogenic Isl1+ cells, esophagi from $Isl1^{Cre}$:$R26^{mT/mG}$ embryos were analyzed at early time points. The emergence of the first *Isl1*-derived mGFP^{+} cells was observed at E12.5, at the anterior end of the esophagus, which coincided with the appearance of *Myf5*+ cells (Figure 3A, inset); a subset of these cells also expressed the upstream cranial mesoderm marker Pitx2 (Figure S3A) and myogenic marker Myod (Figure 3B). By E15.5, actively proliferating *Isl1*-derived Myf5+ myogenic progenitors differentiated into ESMs in an anterior-to-posterior (A-P) developmental gradient (Figure 3C, inset; Figures S3B and S3C). The patterning and differentiation of myogenic progenitors (*Isl1-derived* Myf5+) in the outer layer (ol) preceded that of the inner layer (il) (Figure 3D). Next, to characterize the molecular regulators of the progenitors that seed the ESM, we isolated *Isl1*-derived mGFP+ cells from E12.5 anterior esophagus (Figure 3E) by fluorescence-activated cell sorting (FACS) and evaluated their gene expression profile by qRT-PCR. Transcript analysis of *Isl1*-derived ESM anlagen showed an enrichment of genes encoding pharyngeal mesoderm transcription factors, such as *Tbx1*, *Isl1*, *Msc*, *Tcf21*, and *Six1*, but not the somitic myogenic regulators *Pax3*, *Paraxis*, *Lbx1*, or *Meox1/2* (Figure 3F), attesting to their non-somitic, cranial mesodermal origin.

The patterning of ESM progenitors along the A-P axis of esophagus could occur either by the temporal seeding of progenitors at the anterior esophagus, followed by displacement toward the posterior end, or by spontaneous activation of Isl1/MRFs in a resident progenitor population along the A-P axis of the esophagus. To distinguish between these possibilities, we performed primary myocyte cultures of E12.5 $Isl1^{Cre}$:$R26^{mT/mG}$ esophagus, where the anterior (*Isl1*-derived-GFP+) and posterior (*Isl1*-derived-GFP−) portions were cultured separately for 5 days (Figure 3G). Immunostainings of the myocyte cultures at day 5 showed the presence of myogenic cells (Isl1-derived GFP+/Myod+) only in the anterior, but not in the posterior explant culture (Figure 3H), indicating that spontaneous activation of *Isl1/Mrfs* in a resident progenitor population is not the most plausible mechanism of ESM patterning. To complement this study, we used live imaging of E13.5 $Isl1^{Cre/+}$:$R26^{mT/mG}$ whole-esophagus explants. We found that the *Isl1*-derived mGFP+ cells at the anterior esophagus actively migrated in an A-P direction (Figure S3D; Movies S1 and S2), providing compelling evidence that ESM patterning occurs in a temporal A-P direction after initial seeding at the anterior-most portion of the esophagus.

Esophagus Striated Myogenesis Follows a Unique Fetal Myogenic Program

During skeletal myogenesis, all myogenic progenitors described to date follow a stereotypical sequence of temporal specification, generating embryonic myofibers (E10.5–E13.5), that act as a scaffold, succeeded by fetal myofibers (E14.5–E18.5) and characterized by distinct gene expression patterns and size of differentiated myofibers (Biressi et al., 2007) (Figure 4A). In the esophagus, while the seeding of *Isl1*-derived myogenic progenitors begins at E12.5–E13.5, MyHC+ myofibers appear relatively late (E15.5) (Figures S4A and S4B). Also, ESM formation further extends to postnatal stages, suggesting that ESM differentiation is delayed compared to muscles of the limbs (Kablar et al., 2000; Zhao and Dhoot, 2000). *Isl1* was reported to act as a myogenic repressor that delays MyHC expression in branchiomeric muscle progenitor cells (Nathan et al., 2008), and thus *Isl1* expression might also delay ESM differentiation. To determine whether ESM formation follows the conventional embryonic to fetal myogenic program in spite of the delay in its appearance, we isolated Pax7^{+} progenitors from E15.5 *Tg: Pax7nGFP* esophagus by FACS, and we analyzed transcripts of embryonic and fetal myogenic markers (Mourikis et al., 2012) by qRT-PCR. Interestingly in the ESM progenitors, we observed high transcript abundance of the fetal myogenic markers (*Nfix*, *Socs3*, *Col15a1*, and *CD44*) relative to that of the embryonic markers (*Fgf9*, *Epha4*, and *Slow MyHC*) (Figures 4B and 4C) indicating that these cells are primed for precocious fetal myogenesis. Additionally, myogenic differentiation of these cells in vitro showed a typical fetal morphology, with large multinucleated myofibers similar to those derived from E15.5 forelimb myogenic progenitors (Figure 4D). Importantly, in contrast to other trunk muscles (e.g., Pectoralis major), ESMs did not express the embryonic myofiber-specific Slow Myosin Heavy chain protein (S46) at any developmental time point analyzed (Figures S4C–S4F). Interestingly, we observed that during ESM formation, unlike striated muscles at any other location, the myogenic progenitors were intercalated between the smooth muscle layers, tracing its pre-established pattern (Figure 4E, insets). The unique association of ESM progenitors with the smooth muscle layer suggests that the latter acts as a scaffold to pattern the fetal ESM myofibers in the absence of embryonic fibers (Figure 4F). These findings lead us to propose that striated muscles within the esophagus uniquely bypass embryonic myogenesis and thus use the pre-existing smooth muscle layer as a scaffold for patterning.

Absence of ESMs in *Tbx1*-Null Mutant Embryos

Having established that ESMs are formed by cranial progenitors that follow a unique fetal myogenic program, we sought to identify regulators acting upstream of ESM progenitors. Given the robust transcript abundance of *Tbx1* in the ESM anlage (see Figure 3F) and its critical role in cranial mesoderm-derived myogenesis (Kelly et al., 2004; Sambasivan et al., 2009), we investigated the role of *Tbx1* in ESM formation. Strikingly, ESM and Pax7+ myogenic progenitors were completely absent in all *Tbx1*-null E18.5 fetuses analyzed (Figures 5A and 5B). Sporadic

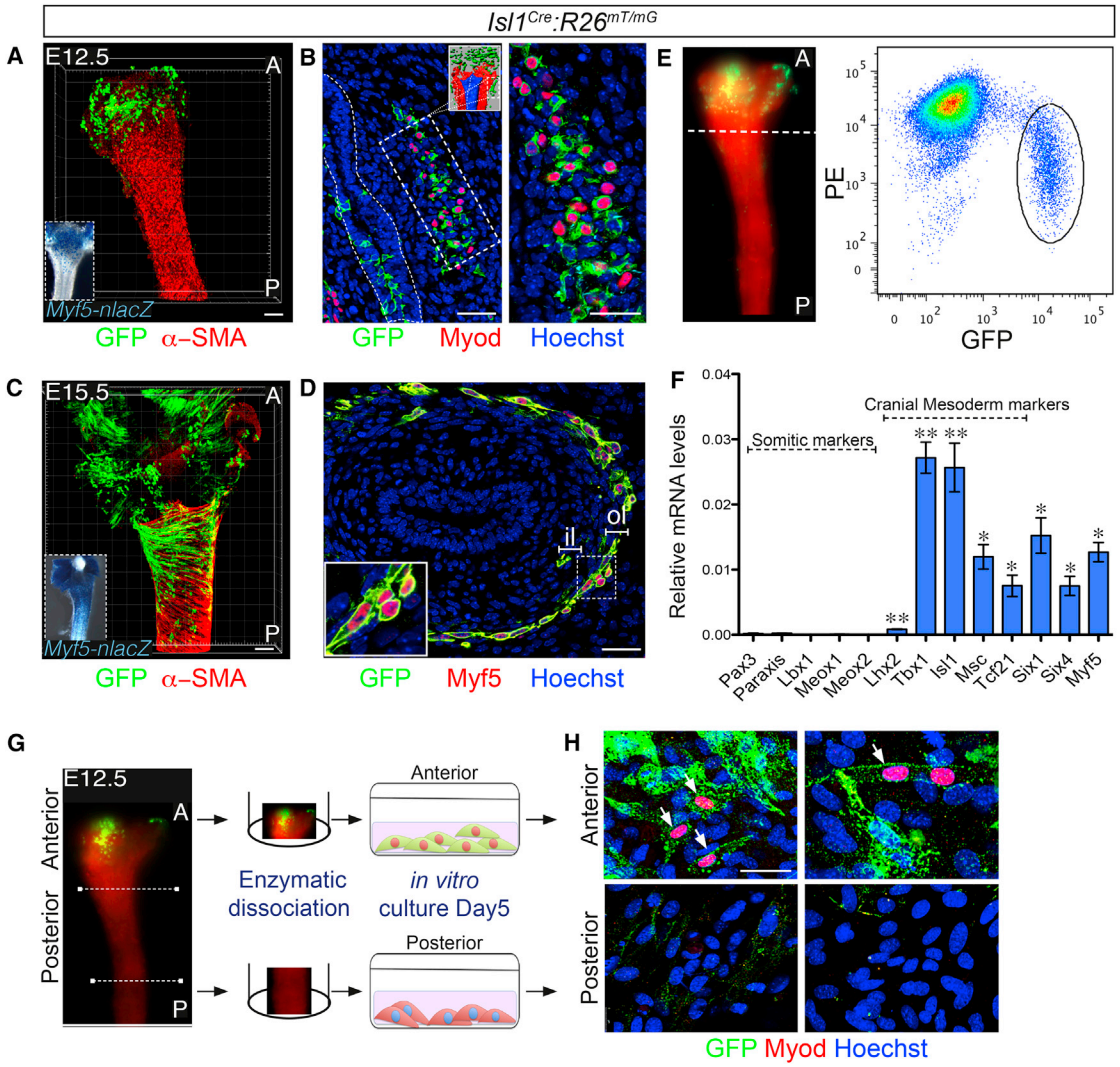

Figure 3. *Isl1*-Derived ESM Progenitors Are Patterned in an A-P Direction, following Initial Seeding at the Anterior End

(A) 3D reconstruction of whole-mount immunostaining of E12.5 *Isl1*$^{Cre/+}$:*R26*$^{mT\text{-}mG/+}$ esophagus for GFP (green, *Isl1*-lineage derived membrane GFP+ cells) and alpha Smooth Muscle Actin (red, α-SMA) (A, anterior; P, posterior); inset E12.5 *Myf5*$^{nlacZ/+}$ esophagus (blue, X-gal) (n = 3).

(B) Immunostaining on sagittal sections of E12.5 *Isl1*$^{Cre/+}$:*R26*$^{mT\text{-}mG/+}$ anterior esophagus (at the level of esophageal opening for GFP (green) and Myod (red). Iso-surface visualization in inset (red, smooth muscle, α-SMA, blue, epithelial lumen) (n = 3).

(C) Same as in (A) for E15.5 *Isl1*$^{Cre/+}$:*R26*$^{mT\text{-}mG/+}$ esophagus.

(D) Immunostaining on the transverse sections of E15.5 *Isl1*$^{Cre/+}$:*R26*$^{mT\text{-}mG/+}$ esophagus for GFP (green) and Myf5 (red); inset, high magnification (il, inner layer; ol, outer layer).

(E) Whole-mount macroscopic image of E12.5 *Isl1*$^{Cre/+}$:*R26*$^{mT\text{-}mG/+}$ esophagus. The dotted line shows the anterior end of esophagus separated for isolation by FACS of *Isl1*-derived GFP+ cells. A profile of the *Isl1*-derived GFP+ cells gated for FACS (right).

(F) qRT-PCR analysis of *Isl*-derived GFP+ cells for somitic and cranial myogenic regulators. All data points are presented as the mean ± SEM (error bars) (n = 3).

(G) Scheme of the experiment. The dotted line demarcates anterior and posterior esophagus isolated from E12.5 *Isl1*$^{Cre/+}$:*R26*$^{mT\text{-}mG/+}$ separated for enzymatic dissociation and ex vivo culture.

(H) Immunostaining of primary culture from anterior (upper) and posterior (lower) segments of esophagus for GFP (green, *Isl1*-lineage derived) and Myod (red, arrowheads) after 5 days in culture (n = 4).

Scale bars represent 50 μm (A and B, left; C and D), 20 μm (B, right; H).

See also Figure S3.

appearance of hypoplastic or normal branchiomeric muscles in *Tbx1*-null embryos is attributed to low-level stochastic *Tbx1*-independent activation of *Mrfs* (Kelly et al., 2004; Kong et al., 2014). However, unlike the other pharyngeal arch-derived muscles, ESMs were totally absent in all *Tbx1* mutants examined with no sporadic appearance of hypoplastic ESM (n = 10). This observation points to an absolute requirement of *Tbx1* for ESM specification and further validates the cranial mesodermal origin of ESM. We note also that a group of *Pax3*-independent *Isl1* lineage-derived laryngeal muscles closely associated with the

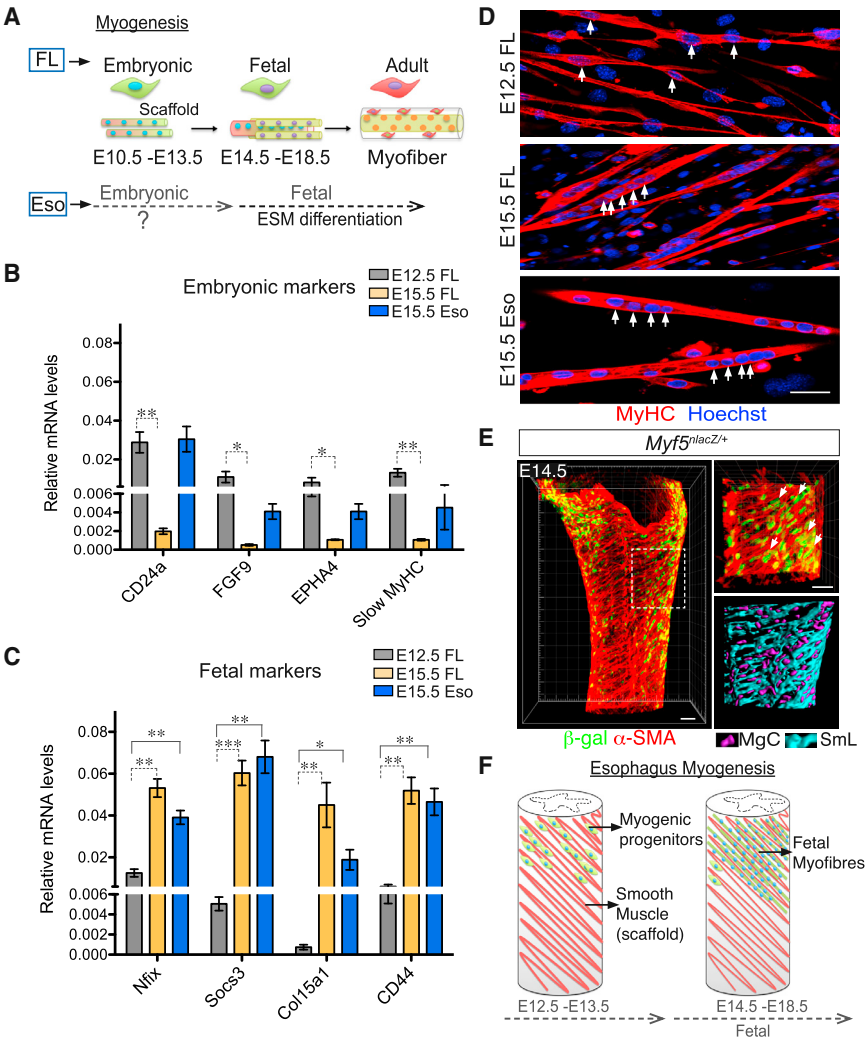

Figure 4. Unique Initiation of Esophageal Striated Myogenesis by Fetal Muscle Progenitors

(A) Scheme depicting the temporal specification of myogenic progenitors for embryonic and fetal myogenesis and the differences between trunk and esophageal muscles.

(B) qRT-PCR for embryonic myogenic markers from Pax7-nGFP cells isolated by FACS from E12.5 forelimbs (embryonic control), E15.5 forelimbs (fetal control), and E15.5 esophagus (test) of *Tg:Pax7-nGFP* embryos.

(C) Same as in (B) for fetal myogenic markers. All data points are presented as the mean ± SEM (error bars) (n = 3).

(D) In vitro myogenic differentiation of Pax7-nGFP cells isolated by FACS from E12.5 forelimbs, E15.5 forelimbs, and E15.5 esophagus of *Tg:Pax7-nGFP* embryos immunostained for MyHC (red). Note that after 7 days in culture, E12.5 forelimb Pax7-nGFP cells form primary myofibers, whereas E15.5 forelimb and esophageal Pax7-nGFP cells form multinucleated secondary myofibers (arrows) (n = 3).

(E) 3D reconstruction of whole-mount immunofluorescence of E14.5 *Myf5*$^{nlacZ/+}$ esophagus for α-SMA (red) and β-gal (green). High magnification (right, top) shows β-gal+ cells (arrows) aligned with smooth muscle fibers (α-SMA+). Iso-surface rendering (right, bottom) of the esophagus model that depicts the unique association of myogenic cells (purple, MgC) and smooth muscle layer (cyan, SmL).

(F) Scheme summarizing how ESMs bypass the scaffold building phase of embryonic myogenesis; myogenic cells intercalate within the smooth muscle layers of the esophagus that provide a putative scaffold for fetal myogenesis.

Scale bars represent 20 μm in (D and E, right), 50 μm in (E, left).

See also Figure S4.

esophagus and trachea (Figure S5A) were consistently absent or severely hypotrophic in *Tbx1* mutants (Figure S5B), indicating a wider role for *Tbx1* outside the esophagus.

Isl1+ Myogenic Cells Fail to Colonize Esophagus in *Tbx1*-Null Mutants

We hypothesized that the absence of ESM and the associated muscles in *Tbx1*-null mice could be attributed either to a failure of Isl1+ progenitor cells to arrive at the cranial end of the esophagus or the inability of the *Tbx1*-null Isl1+ progenitors to activate *Mrfs* in the esophagus. Analysis of E12.5 *Tbx1* mutants showed the presence of Isl1+ progenitors in the surrounding pharyngeal mesoderm. However, the wing-like extension of Isl1+ progenitors proximal to the anterior esophagus was entirely missing in mutants compared to control embryos, suggesting that in the absence of *Tbx1*, Isl1+ progenitors fail to arrive and seed the anterior esophagus (Figures 5C and 5D). To determine the epistatic relationship between *Tbx1* and *Isl1*, we generated *Tbx1* mutant embryos coupled with *Isl1* genetic lineage tracing. Strikingly, analysis of E18.5 embryos showed a complete absence of *Isl1*-derived facial and lower mandibular muscles in *Tbx1*-null mutants (*Tbx1*$^{-/-}$*:Isl1*$^{Cre/+}$*:R26*$^{mT\text{-}mG/+}$*:Myf5*$^{nlacZ/+}$) compared to control embryos (*Tbx1*$^{+/-}$*:Isl1*$^{Cre/+}$*:R26*$^{mT\text{-}mG/+}$*:Myf5*$^{nlacZ/+}$) (Figures 5E and 5F, insets; Figure S5C). Furthermore, *Isl1*-derived mGFP+ myogenic cells (β-gal+) and ESM (MyHC+) were completely absent from the *Tbx1* mutant esophagus (Figures 5E and 5F), confirming that *Tbx1* acts upstream in *Isl1*-derived progenitors and is required for the seeding of the esophagus by Isl1+ myogenic progenitors. We note that in the esophagus of *Tbx1* mutant embryos, despite the absence of ESM, the expression pattern of the smooth muscle layer (α-smooth muscle actin), lamina propria/connective tissue (Tcf4), innervation (Tuj1), and endothelial vascular cells (CD31) all appeared unperturbed (Figure S5D), suggesting that *Tbx1* is likely to act cell autonomously in Isl1+ ESM progenitors. In the light of our findings that ESM progenitors express *Mesp1*, *Tbx1*, and *Isl1*, as do CpM progenitors that give rise to branchiomeric muscles and second heart field-derived myocardium, we propose that esophageal and associated striated muscles constitute a distinct third myogenic derivative of pharyngeal mesoderm.

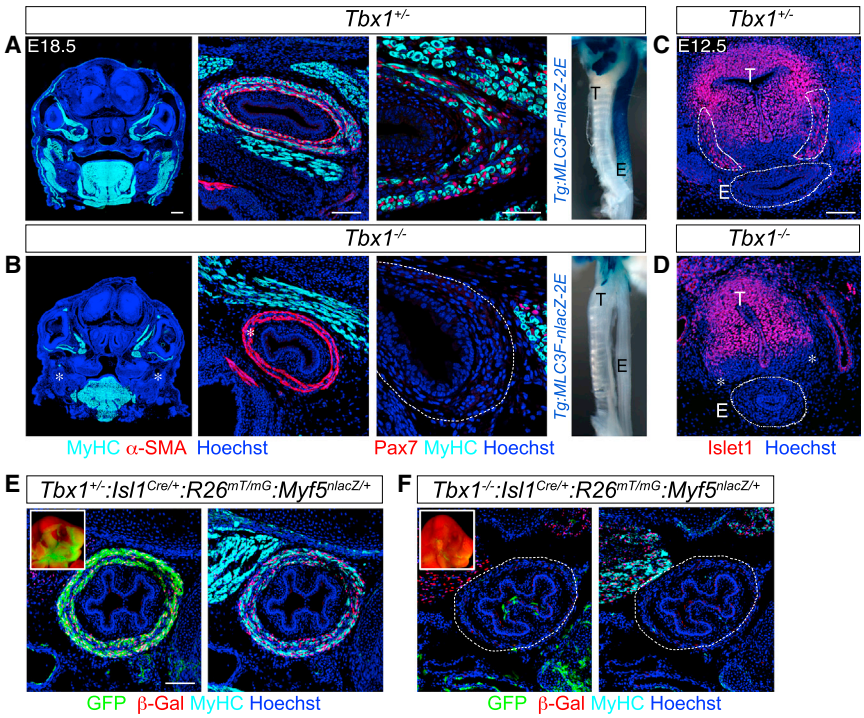

Figure 5. Failure of Esophagus Striated Myogenesis in *Tbx1* Mutant Mice

(A) Immunofluorescence staining of E18.5 control (*Tbx1*$^{+/-}$) head muscles (cyan, MyHC) and esophagus muscles (cyan, MyHC; red, α-SMA; or red, Pax7). Note that the *Tbx1*$^{-/-}$ esophagus lacks differentiated MyHC+ fibers and Pax7+ satellite cells (n = 10). X-gal staining on whole-mount esophagus of control (*Tbx1*$^{+/-}$*::Tg:MLC3F-nlacZ-2E*) (right).

(B) Same as in (A) for mutant (*Tbx1*$^{-/-}$). Note the complete absence of masticatory and mandibular (asterisk, right) and esophagus striated muscles (asterisk, right) in the *Tbx1* null mutant (n = 10).

(C and D) Immunostaining of E12.5 trunk transverse section for Islet1 (red) (E, esophagus; T, trachea) in control (C) and *Tbx1*$^{-/-}$ (D) embryos. Note the lack of lateral *Isl1*-expressing cells between the trachea and esophagus (asterisk) in *Tbx1*$^{-/-}$ mutant. The dashed line demarcates wing-like expression of Isl1+ cells in the anterior esophagus of control embryos. Dotted line demarcates the esophagus (n = 3).

(E) Whole-mount view of dissected embryo (head, inset) and immunofluorescence staining on transverse sections of anterior esophagus of control E18.5 (*Tbx1*$^{+/-}$*:Isl1*$^{Cre/+}$*:R26*$^{mT\text{-}mG/+}$*:Myf5*$^{nlacZ/+}$) embyo for GFP (green, *Isl1*-Cre lineage derived), β-gal (red), and MyHC (cyan).

(F) Same as in (E) for mutant (*Tbx1*$^{-/-}$*:Isl1*$^{Cre/+}$*:R26*$^{mT\text{-}mG/+}$*:Myf5*$^{nlacZ/+}$). Note the near-complete absence of GFP+ facial muscles in the mutant (see inset). Esophagi of mutants completely lack *Isl1*-derived myogenic cells (n = 2).

Scale bars represent 200 μm (A and B, left), 50 μm (A and B; right and middle, C, D, E, and F).

See also Figure S5.

Isl1+ Progenitors Are Not Found in Close Proximity to the Developing Chicken Esophagus

Lineage studies have shown that Isl1+ CpM cells contribute to facial and intermandibular branchiomeric muscles in avians, similar to that in mouse (Nathan et al., 2008; Tzahor and Evans, 2011). Given our observation that the ESM is also a derivative of the Isl1+ CpM, we analyzed the development of the esophagus in chick. Analysis of HH36 stage chick and adult quail esophagus and crop (an esophageal modification) for MyHC and α-SMA expression showed that, unlike in mouse, the muscularis externae of the chick and quail esophagi were entirely devoid of striated muscles and consisted only of smooth muscle as previously reported (Shiina et al., 2005). Remarkably, comparative analysis of different developmental time points in mouse and chick embryos showed that Isl1+ progenitors (particularly the wing-like extension) were absent in the region proximal to the developing esophagus in the chick as opposed to that in the mouse (Figures 6A–6D, S6A, and S6B). This situation is strikingly similar to that observed in *Tbx1*-null mice (Figure 5D; see above). Taken together, these data indicate that *Tbx1* and *Isl1* are critical determinants of ESM fate; in their absence, ESM myogenesis fails to occur (Figure 6E).

DISCUSSION

Esophageal striated muscles undergo peristalsis to propel ingested food to the stomach. Perturbations in ESM function lead to dysphagia and other disorders that impair swallowing. Given its location in the trunk, previous studies, including lineage-tracing experiments, lead to the proposal that esophageal striated muscles (ESMs) originate from somites (see Minchin et al., 2013).

Here, we used extensive lineage tracing, *Pax3* (somitic), *Mesp1*, and *Isl1* (cranial), *Pax3* and *Tbx1* mouse mutants, high-resolution image analysis and a neuronal-specific marking (Tuj1) to assess the contribution of *Pax3*-derived somitic progenitors to the striated muscles of the esophagus. We demonstrate that ESMs are cranial mesodermal in origin and that *Pax3*-derived cells do not contribute to this myogenic compartment, but rather to the innervation of the esophagus. This is consistent with previous reports that *Pax3* is also expressed by the migratory neural crest cells and give rise to enteric nervous system among other cell types in vertebrate embryos (Lang et al., 2000).

We define here, for the first time, a genetic regulatory network for ESM in cardiopharyngeal mesoderm, where *Tbx1* acts upstream of *Isl1* to establish ESM in a biphasic manner, first to seed the base of the oral cavity with pharyngeal-derived progenitors, followed by a posterior migration of these progenitors along the esophagus to colonize this structure. In *Tbx1*-null mutants, *Isl1* progenitors fail to colonize esophagus and lack ESMs, completely suggesting that *Tbx1* is critical to initiate myogenic fate in Isl1+ ESM progenitors and acts genetically upstream of *Isl1*. A recent report has demonstrated the cell-autonomous role of *Tbx1* in cell survival and cell fate in pharyngeal mesoderm that forms the masticatory muscles (Kong et al., 2014). Given our observation that Isl1+ progenitors persist in *Tbx1* mutants and

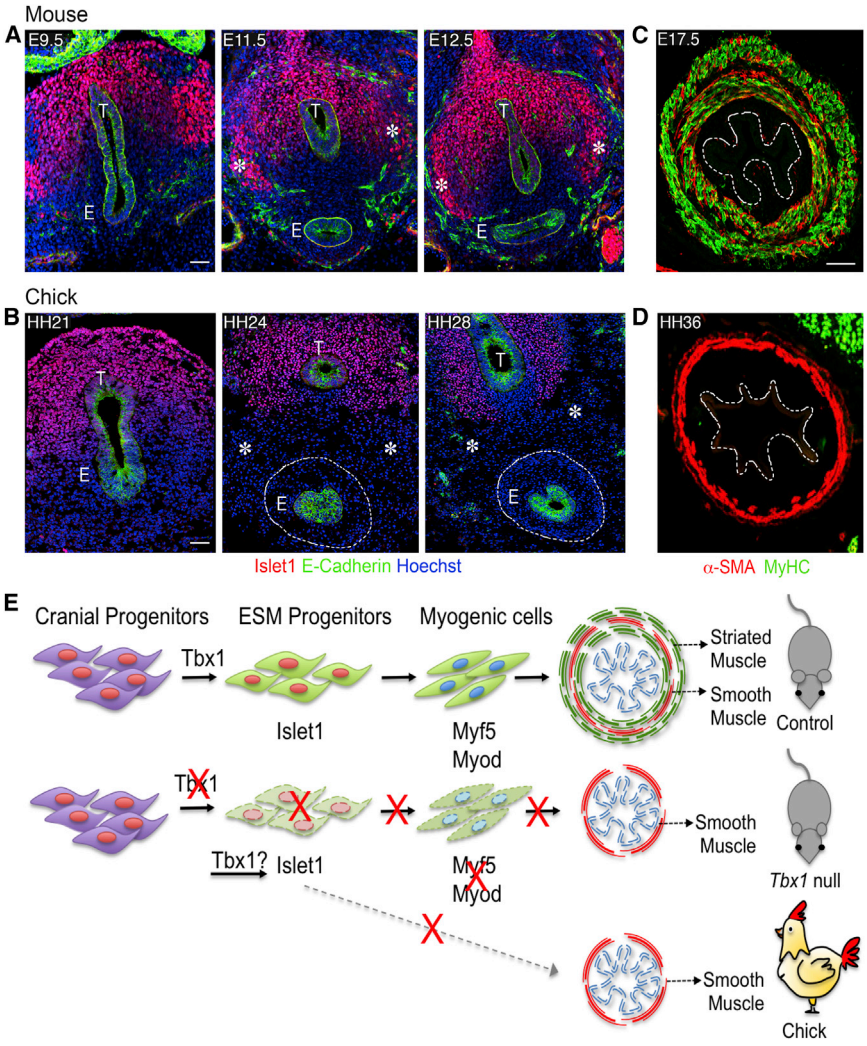

Figure 6. Isl1-Expressing Progenitors Do Not Colonize the Developing Esophagus in Chicken

(A) Immunostaining of E9.5, E11.5, and E12.5 mouse trunk transverse sections for Islet1 (red) and E-cadherin (green) (n = 3).

(B) Same as in (A) for HH21, HH24, and HH28 chick trunk transverse sections. Note that the lateral Isl1 wing-like extensions are completely absent in the chick (*asterisk) (n = 3). The dotted line outlines the esophagus (E, esophagus; T, trachea).

(C) Immunostaining of E17.5 mouse esophagus transverse section for α-SMA (red) and MyHC (green).

(D) Same as in (C) for HH36 chick esophagus transverse section. Note that the chick esophagus lacks striated muscles (n = 3). The dotted line marks the esophagus lumen.

(E) Scheme showing that *Tbx1* acts upstream of *Isl1* in esophageal myogenic progenitors, and in the absence of *Tbx1* and *Isl1* expression, ESMs are not established.

Scale bar represents 100 μm (A and B), 50 μm (C and D).

See also Figure S6.

are not eliminated completely from the pharyngeal mesoderm proximal to the trachea and esophagus (only the wing-like expression pattern of Isl1+ is missing), it is likely that the ESM phenotype observed is due to a cell-autonomous role of *Tbx1* in determining the myogenic fate of Isl1+ ESM progenitors. These observations warrant further investigations, and future studies using conditional mutation of *Tbx1* will help in elucidating the precise role of this gene in ESM development.

Unlike other craniofacial muscles, the myogenic differentiation of ESM progenitors occurs late in embryonic development (E15.5) and extends through postnatal stages. Conventionally, striated myogenesis in the body follows a temporal specification program in which embryonic myofibers are first formed, and these act as a scaffold for the later differentiating fetal myofibers. Intriguingly, we observed that striated muscles in the esophagus are established exclusively by fetal myofibers, thereby bypassing the conventional embryonic program. This ontology is novel and has not been noted for other skeletal muscles and also raises the question of the nature of the scaffold for fetal myogenesis. Our observations on the patterning of myogenic progenitors to the esophagus wall lead us to propose that the pre-patterned smooth muscle fibers could provide the scaffold for ESM patterning. Functional studies will be extended to dissect the role of smooth muscles in the pattering of ESM. The esophageal wall in birds and reptiles lacks striated musculature and is lined uniquely by smooth muscles. Interestingly, we observed that unlike the mouse, Isl1+ progenitors in the chick are not established in the first phase to seed the oropharyngeal region, thus pointing to a possible regulatory mechanism explaining the lack of esophageal striated muscles in avians. We hypothesize that the absence of Isl1+ myogenic progenitors in the anterior chick esophagus could result from either of the following: (1) the cell-autonomous gene regulatory network that operates in Isl1+ mouse ESM progenitors is repressed/altered in the chick, or (2) the pro-migratory and pro-myogenic signaling milieu, present in the mouse esophagus, is not duplicated in the chick, and hence the proposed migration of the Isl1 progenitors and subsequent myogenic differentiation to ESM does not occur. These hypotheses will be tested in future studies.

The loss of ESM in birds opens new questions concerning the evolution of the vertebrate pharynx. Evolution of chordates involved the development of an enlarged pharynx with modified pharyngeal clefts that act as a filter to collect food internally (Glenn Northcutt, 2005). Previous studies have suggested a possible co-evolution of circulatory and feeding functions in early chordates (*Ciona intestinalis*), where the siphon muscles in the anterior gut share a common origin with the cardiac lineage (Stolfi et al., 2010). Notably, two axes have been defined for cardiopharyngeal progenitor cell fates: craniofacial muscles and cardiac progenitor cells of the second heart field (Diogo et al., 2015; Grifone and Kelly, 2007; Tzahor and Evans, 2011). Our

studies point to the ESM as a novel third derivative of cardiopharyngeal mesoderm that has been forfeited in avians. We hypothesize that the absence of mastication in avians could have supported the evolution of a uniquely smooth muscle lined esophagus with greater distensibility for rapid ingestion of coarse food. Further, given the common origins of siphon and cardiac lineages in tunicates, it is possible that this branch point that is homologous to the ESM is evolutionary more ancient than craniofacial muscles.

Taken together, our results clearly demonstrate a cranial mesoderm origin of striated muscle of the esophagus that is located in the trunk. In a previous study using *Z/AP* reporter mice, Kaede lineage tracing, and *pax3b* morpholinos in zebrafish, the ESM was reported to be a derivative of *Pax3*-derived migratory somitic progenitors (Minchin et al., 2013). However, our results demonstrate that the *Pax3* lineage does not contribute to ESM. We attribute the discrepancies to two factors. First, analyzing the esophagi of $Pax3^{Cre/+}$:$R26^{mT/mG}$ embryos, we highlight the fact that *Pax3* derivatives contributing to the enteric neurons of the esophagus are found in close proximity to the myogenic cells and could be mistaken for myogenic cells. By providing high-resolution analysis and 3D reconstructions, we show that that the *Pax3* lineage does not contribute to the ESM in mice. Second, with the increasing concerns on the use of Morpholinos (Kok et al., 2015; Schulte-Merker and Stainier, 2014), it would be important to examine mutants of *pax3b* to conclusively demonstrate its role in ESM formation in zebrafish. Indeed, a "small head phenotype" was noted in *pax3b* MO1 morpholino zebrafish mutants (Minchin et al., 2013). However, our analysis of E18.5 *Pax3* mutant mice conclusively demonstrates that *Pax3*-derived migratory myogenic progenitors are not required for ESM formation in mice.

Finally, understanding the developmental origin of ESM has important clinical ramifications, as *TBX1* haploinsufficiency is implicated in DiGeorge syndrome. These patients exhibit cardiovascular and craniofacial abnormalities that include problems with swallowing (Rózsai et al., 2009). Our finding that the ESMs are a third derivative of the cardiopharyngeal mesoderm and critically require *Tbx1* prompts investigations of defects in ESM, which may underlie dysphagia and feeding disorders in these patients (Eicher et al., 2000).

EXPERIMENTAL PROCEDURES

Animals

Animals were handled as per European Community guidelines, and the ethics committee of the Institut Pasteur (CTEA) approved protocols. Cre recombinase, $Pax3^{Cre/+}$ (Engleka et al., 2005), $Mesp1^{Cre/+}$ (Saga et al., 1999), and $Isl1^{Cre/+}$ (Srinivas et al., 2001) and reporter mouse lines $R26R^{mT/mG}$ (Muzumdar et al., 2007), $Pax7^{GPL}$ (Sambasivan et al., 2013), $Myf5^{nLacZ/+}$ (Tajbakhsh et al., 1996), *Tg: MLC3F-lacZ-2E* (Kelly et al., 1995), and *Z/AP* (Lobe et al., 1999) were described previously. Mice carrying the $Tbx1^{tm1pa}$ allele (referred to as $Tbx1^{-/-}$) were described previously (Jerome and Papaioannou, 2001). To generate experimental embryos for $Tbx1^{-/-}$, *Isl1*, and *Myf5* lineage tracing ($Tbx1^{-/-}$: $Isl1^{Cre/+}$: $R26R^{mT/mG/+}$: $Myf5^{nlacZ/+}$), we crossed $Tbx1^{+/-}$: $Isl1^{Cre/+}$: $Myf5^{nlacZ/+}$ mice with $Tbx1^{+/-}$: $R26R^{mT/mG}$ male/female mice.

Embryos

Mouse embryos were collected between embryonic day 12.5 (E12.5) and E18.5, with noon on the day of the vaginal plug considered as E0.5. Fertilized chicken eggs from commercial sources were incubated at 38.5°C to the appropriate Hamburger Hamilton (HH) stage in a humidified incubator. Adult quail were euthanized using an overdose of sodium pentobarbitone (150 mg/kg bodyweight) via intracoelomic injection.

Histology

For cryosections, embryos were fixed in 4% paraformaldehyde and 0.1% Triton X-100 (1–2 hr), washed overnight in 1× PBS/0.1% Tween-20, equilibrated in 15% sucrose/PBS overnight, embedded in OCT, frozen in liquid nitrogen, and sectioned at 16- to 20-μm thickness.

X-Gal Staining

Whole-mount samples or cryosections were analyzed for β-galactosidase (β-gal) activity as described previously (Comai et al., 2014), and tissue sections were post-fixed in 4% PFA and counterstained with 2% aqueous eosin. For immunohistochemistry on MyHC (rabbit, 1/750), sections were treated in 0.3% hydrogen peroxidase in 1× PBS to block endogenous peroxidase activity, and labeling was revealed with an anti-Rb HRP antibody (Vector, PI-1000, 1/1,500) and DAB (3, 3′-diaminobenzidine) peroxidase (HRP) substrate kit, in accordance with the manufacturer's instructions (Vector Laboratories, SK-4100).

Immunofluorescence Staining

Immunostaining on sections was performed as previously described (Comai et al., 2014). For whole-mount immunostaining, esophagi at specific time points were micro-dissected from PFA-fixed embryos, washed in PBS, and incubated in blocking buffer (3% goat serum, 1% BSA, and 0.5% Triton X-100 in 1× PBS) for 1 hr at 4°C. The tissue was then incubated in primary antibody in the blocking buffer for 4–5 days at 4°C on a roller. The tissue was washed extensively for 1–2 hr in 1× PBS/0.1% Tween-20 and then incubated in Fab′ secondary antibody overnight at 4°C on a roller. The tissue was washed extensively and then cleared for 3D imaging by SCALE (Hama et al., 2011) or BABB (Yokomizo et al., 2012) protocols as described previously. Antibodies used include the following: GFP (chicken, Abcam, 13970; 1/1,000), Pax7 (mouse monoclonal, DSHB; 1/20), Myod (mouse monoclonal, Dako, M3512; 1/50), Myogenin (mouse monoclonal, DSHB, F5D; 1/100), Myf5 (rabbit, Santa-Cruz Biotechnology, sc-302; 1/250), MyHC (rabbit, kindly provided by G. Cossu, 1/750; mouse monoclonal MF20, DSHB, 1/30), Islet1 (mouse monoclonal, DSHB, 40.2D6; 1/750), Pitx2 (rabbit, kindly provided by J. Drouin, 1/300), alpha smooth muscle actin (rabbit, Abcam, 1/1,000), Desmin (mouse monoclonal, DAKO M0760, 1/200), avian slow myosin heavy chain (mouse monoclonal DSHB S46, 1/200), β-galactoside (rabbit polyclonal, MP Biomedicals 08559761), and E-cadherin (Mouse, 1/500, BD Biosciences).

Imaging

Images were acquired using the following systems: a Zeiss Axio-plan equipped with an Apotome and ZEN software (Carl Zeiss), a Leica SPE confocal and Leica Application Suite (LAS) software or a LSM 700 laser-scanning confocal microscope and ZEN software (Carl Zeiss). All images were assembled in Adobe Photoshop and InDesign (Adobe Systems). Volume-rendered 3D reconstruction and Iso-surface rendering were performed on the z series using Imaris software (Bitplane).

Primary Cell Culture

For primary myocyte culture of anterior and posterior esophagi, E12.5 $Isl1^{Cre/+}$: $R26^{mT/mG}$ esophagi were micro-dissected in cold DMEM under a Zeiss SteREO Discovery V20 microscope. Isl1-GFP+ anterior part and Isl1-GFP- posterior part were collected in separate tubes and processed with enzymatic digestion mix 0.25% Trypsin (15090-046,GIBCO) and 10 μg/ml of DNase I (04536282001, Roche) in DMEM (31966, GIBCO). Samples were incubated at 37°C for 5 min and resuspended by gently pipetting up and down 10–15 times using a plastic Pasteur pipette and incubated for an additional 5 min. Suspension by pipetting was repeated, and digests were passed through a 40-μm filter, and digestion was stopped with 5 ml of Foetal Bovine Serum (GIBCO). Cells were spun 15 min at 500 rcf at 4°C, and the pellets were resuspended in 2 ml of culture media (20% FBS and 1% Penicillin-Streptomycin DMEM + Glutamax (GIBCO) and Ultraser and cultured on matrigel-coated (354234, BD Biosciences) plates at 37°C or suspended

in DMEM/2% FBS to be processed for FACS. For in vitro myogenic differentiation, *Tg:Pax7-nGFP* E12.5 and E15.5 forelimbs and E15.5 esophagi were microdissected in cold DMEM under sterile conditions and processed as above. GFP+ cells from FACS were collected in (20%FBS and 1% Penicillin-Streptomycin DMEM + Glutamax (GIBCO) and Ultraser (PALL, Life Sciences) and cultured on matrigel-coated (354234, BD Biosciences) plates at 37°C.

qRT-PCR

Total RNA was extracted from cells isolated by FACS directly into cell lysis buffer (RLT) of a QIAGEN RNAeasy Micropurification Kit. The equivalent of 1.5×10^3 cells was used/transcript amplified. cDNA was prepared by random-primed reverse transcription (Super-Script II, Invitrogen, 18064-014), and real-time PCR was done using SYBR Green Universal Mix (Roche, 13608700) StepOne-Plus, Perkin-Elmer (Applied Biosystems). *Gapdh* transcript levels were used for normalizations of each target (= ΔCT). At least three biological replicates were used for each condition (ΔΔCT) method (Schmittgen and Livak, 2008). For SYBR-Green, custom primers were designed using the Primer3Plus online software. Serial dilutions of total cDNA were used to calculate the amplification efficiency of each primer set according to the equation: $E = 10 - 1/\text{slope}$. Primer sequences are described in the Supplemental Experimental Procedures. Primer sequences of embryonic and fetal myogenic markers were described previously (Mourikis et al., 2012).

Statistics

All experiments were carried out on a minimum of three embryos, except where stated otherwise. The graphs were plotted and statistical analyses were performed using GraphPad Prism software. All data points are presented as the mean ± SEM (error bars). The Student's t test (two-tailed, unpaired) was applied in all cases (*$p < 0.05$; **$p < 0.01$; ***$p < 0.001$).

SUPPLEMENTAL INFORMATION

Supplemental Information includes Supplemental Experimental Procedures, six figures, and two movies and can be found with this article online at http://dx.doi.org/10.1016/j.devcel.2015.07.003.

AUTHOR CONTRIBUTIONS

S.G., R.G.K., and S.T. conceived of and designed the experiments and wrote the manuscript. S.G. performed most of the experiments. G.C. performed immunostaining and image processing, and R.S. initiated the study. A.F. performed immunostainings. All authors interpreted the results and read and approved the final manuscript.

ACKNOWLEDGMENTS

We acknowledge funding support from the Institut Pasteur, Association Française contre le Myopathies, Agence Nationale de la Recherche (Laboratoire d'Excellence Revive, Investissement d'Avenir; ANR-10-LABX-73), the Association pour la Recherche sur le Cancer, and the Fondation pour la Recherche Médicale. We acknowledge the service of Pasteur Imaging platform (PFID) and Pasteur Flow Cytometry Platform. We thank C. Cimper for technical assistance, J. Gros for providing chick eggs and adult quail, and the members of the lab for helpful discussions.

Received: February 10, 2015
Revised: June 8, 2015
Accepted: July 10, 2015
Published: September 17, 2015

REFERENCES

Biressi, S., Molinaro, M., and Cossu, G. (2007). Cellular heterogeneity during vertebrate skeletal muscle development. Dev. Biol. *308*, 281–293.

Comai, G., Sambasivan, R., Gopalakrishnan, S., and Tajbakhsh, S. (2014). Variations in the efficiency of lineage marking and ablation confound distinctions between myogenic cell populations. Dev. Cell *31*, 654–667.

Daston, G., Lamar, E., Olivier, M., and Goulding, M. (1996). Pax-3 is necessary for migration but not differentiation of limb muscle precursors in the mouse. Development *122*, 1017–1027.

Diogo, R., Kelly, R.G., Christiaen, L., Levine, M., Ziermann, J.M., Molnar, J.L., Noden, D.M., and Tzahor, E. (2015). A new heart for a new head in vertebrate cardiopharyngeal evolution. Nature *520*, 466–473.

Eicher, P.S., McDonald-Mcginn, D.M., Fox, C.A., Driscoll, D.A., Emanuel, B.S., and Zackai, E.H. (2000). Dysphagia in children with a 22q11.2 deletion: unusual pattern found on modified barium swallow. J. Pediatr. *137*, 158–164.

Engleka, K.A., Gitler, A.D., Zhang, M., Zhou, D.D., High, F.A., and Epstein, J.A. (2005). Insertion of Cre into the Pax3 locus creates a new allele of Splotch and identifies unexpected Pax3 derivatives. Dev. Biol. *280*, 396–406.

Glenn Northcutt, R. (2005). The new head hypothesis revisited. J. Exp. Zoolog. B Mol. Dev. Evol. *304*, 274–297.

Grifone, R., and Kelly, R.G. (2007). Heartening news for head muscle development. Trends Genet. *23*, 365–369.

Hama, H., Kurokawa, H., Kawano, H., Ando, R., Shimogori, T., Noda, H., Fukami, K., Sakaue-Sawano, A., and Miyawaki, A. (2011). Scale: a chemical approach for fluorescence imaging and reconstruction of transparent mouse brain. Nat. Neurosci. *14*, 1481–1488.

Harel, I., Nathan, E., Tirosh-Finkel, L., Zigdon, H., Guimarães-Camboa, N., Evans, S.M., and Tzahor, E. (2009). Distinct origins and genetic programs of head muscle satellite cells. Dev. Cell *16*, 822–832.

Jerome, L.A., and Papaioannou, V.E. (2001). DiGeorge syndrome phenotype in mice mutant for the T-box gene, Tbx1. Nat. Genet. *27*, 286–291.

Kablar, B., Tajbakhsh, S., and Rudnicki, M.A. (2000). Transdifferentiation of esophageal smooth to skeletal muscle is myogenic bHLH factor-dependent. Development *127*, 1627–1639.

Kassar-Duchossoy, L., Gayraud-Morel, B., Gomès, D., Rocancourt, D., Buckingham, M., Shinin, V., and Tajbakhsh, S. (2004). Mrf4 determines skeletal muscle identity in Myf5:Myod double-mutant mice. Nature *431*, 466–471.

Kassar-Duchossoy, L., Giacone, E., Gayraud-Morel, B., Jory, A., Gomès, D., and Tajbakhsh, S. (2005). Pax3/Pax7 mark a novel population of primitive myogenic cells during development. Genes Dev. *19*, 1426–1431.

Kelly, R., Alonso, S., Tajbakhsh, S., Cossu, G., and Buckingham, M. (1995). Myosin light chain 3F regulatory sequences confer regionalized cardiac and skeletal muscle expression in transgenic mice. J. Cell Biol. *129*, 383–396.

Kelly, R.G., Jerome-Majewska, L.A., and Papaioannou, V.E. (2004). The del22q11.2 candidate gene Tbx1 regulates branchiomeric myogenesis. Hum. Mol. Genet. *13*, 2829–2840.

Kilic, S.S., Gurpinar, A., Yakut, T., Egeli, U., and Dogruyol, H. (2003). Esophageal atresia and tracheo-esophageal fistula in a patient with Digeorge syndrome. J. Pediatr. Surg. *38*, E21–E23.

Kok, F.O., Shin, M., Ni, C.W., Gupta, A., Grosse, A.S., van Impel, A., Kirchmaier, B.C., Peterson-Maduro, J., Kourkoulis, G., Male, I., et al. (2015). Reverse genetic screening reveals poor correlation between morpholino-induced and mutant phenotypes in zebrafish. Dev. Cell *32*, 97–108.

Kong, P., Racedo, S.E., Macchiarulo, S., Hu, Z., Carpenter, C., Guo, T., Wang, T., Zheng, D., and Morrow, B.E. (2014). Tbx1 is required autonomously for cell survival and fate in the pharyngeal core mesoderm to form the muscles of mastication. Hum. Mol. Genet. *23*, 4215–4231.

Lang, D., Chen, F., Milewski, R., Li, J., Lu, M.M., and Epstein, J.A. (2000). Pax3 is required for enteric ganglia formation and functions with Sox10 to modulate expression of c-ret. J. Clin. Invest. *106*, 963–971.

Lescroart, F., Hamou, W., Francou, A., Theveniau-Ruissy, M., Kelly, R.G., and Buckingham, M. (2015). Clonal analysis reveals a common origin between nonsomite-derived neck muscles and heart myocardium. Proc. Natl. Acad. Sci. U.S.A. *112*, 1446–1451.

Lobe, C.G., Koop, K.E., Kreppner, W., Lomeli, H., Gertsenstein, M., and Nagy, A. (1999). Z/AP, a double reporter for cre-mediated recombination. Dev. Biol. *208*, 281–292.

Minchin, J.E., Williams, V.C., Hinits, Y., Low, S., Tandon, P., Fan, C.M., Rawls, J.F., and Hughes, S.M. (2013). Oesophageal and sternohyal muscle fibres are novel Pax3-dependent migratory somite derivatives essential for ingestion. Development *140*, 2972–2984.

Mourikis, P., Gopalakrishnan, S., Sambasivan, R., and Tajbakhsh, S. (2012). Cell-autonomous Notch activity maintains the temporal specification potential of skeletal muscle stem cells. Development *139*, 4536–4548.

Muzumdar, M.D., Tasic, B., Miyamichi, K., Li, L., and Luo, L. (2007). A global double-fluorescent Cre reporter mouse. Genesis *45*, 593–605.

Nathan, E., Monovich, A., Tirosh-Finkel, L., Harrelson, Z., Rousso, T., Rinon, A., Harel, I., Evans, S.M., and Tzahor, E. (2008). The contribution of Islet1-expressing splanchnic mesoderm cells to distinct branchiomeric muscles reveals significant heterogeneity in head muscle development. Development *135*, 647–657.

Patapoutian, A., Wold, B.J., and Wagner, R.A. (1995). Evidence for developmentally programmed transdifferentiation in mouse esophageal muscle. Science *270*, 1818–1821.

Relaix, F., Rocancourt, D., Mansouri, A., and Buckingham, M. (2004). Divergent functions of murine Pax3 and Pax7 in limb muscle development. Genes Dev. *18*, 1088–1105.

Relaix, F., Rocancourt, D., Mansouri, A., and Buckingham, M. (2005). A Pax3/Pax7-dependent population of skeletal muscle progenitor cells. Nature *435*, 948–953.

Rishniw, M., Xin, H.B., Deng, K.Y., and Kotlikoff, M.I. (2003). Skeletal myogenesis in the mouse esophagus does not occur through transdifferentiation. Genesis *36*, 81–82.

Romer, A.I., Singh, J., Rattan, S., and Krauss, R.S. (2013). Smooth muscle fascicular reorientation is required for esophageal morphogenesis and dependent on Cdo. J. Cell Biol. *201*, 309–323.

Rózsai, B., Kiss, A., Csábi, G., Czakó, M., and Decsi, T. (2009). Severe dystrophy in DiGeorge syndrome. World J. Gastroenterol. *15*, 1391–1393.

Rudnicki, M.A., Schnegelsberg, P.N., Stead, R.H., Braun, T., Arnold, H.H., and Jaenisch, R. (1993). MyoD or Myf-5 is required for the formation of skeletal muscle. Cell *75*, 1351–1359.

Saga, Y., Miyagawa-Tomita, S., Takagi, A., Kitajima, S., Miyazaki, Ji., and Inoue, T. (1999). MesP1 is expressed in the heart precursor cells and required for the formation of a single heart tube. Development *126*, 3437–3447.

Saga, Y., Kitajima, S., and Miyagawa-Tomita, S. (2000). Mesp1 expression is the earliest sign of cardiovascular development. Trends Cardiovasc. Med. *10*, 345–352.

Sambasivan, R., Gayraud-Morel, B., Dumas, G., Cimper, C., Paisant, S., Kelly, R.G., and Tajbakhsh, S. (2009). Distinct regulatory cascades govern extraocular and pharyngeal arch muscle progenitor cell fates. Dev. Cell *16*, 810–821.

Sambasivan, R., Comai, G., Le Roux, I., Gomès, D., Konge, J., Dumas, G., Cimper, C., and Tajbakhsh, S. (2013). Embryonic founders of adult muscle stem cells are primed by the determination gene Mrf4. Dev. Biol. *381*, 241–255.

Schmittgen, T.D., and Livak, K.J. (2008). Analyzing real-time PCR data by the comparative C(T) method. Nat. Protoc. *3*, 1101–1108.

Schulte-Merker, S., and Stainier, D.Y. (2014). Out with the old, in with the new: reassessing morpholino knockdowns in light of genome editing technology. Development *141*, 3103–3104.

Sheehan, N.J. (2008). Dysphagia and other manifestations of oesophageal involvement in the musculoskeletal diseases. Rheumatology (Oxford) *47*, 746–752.

Shiina, T., Shimizu, Y., Izumi, N., Suzuki, Y., Asano, M., Atoji, Y., Nikami, H., and Takewaki, T. (2005). A comparative histological study on the distribution of striated and smooth muscles and glands in the esophagus of wild birds and mammals. J. Vet. Med. Sci. *67*, 115–117.

Srinivas, S., Watanabe, T., Lin, C.S., William, C.M., Tanabe, Y., Jessell, T.M., and Costantini, F. (2001). Cre reporter strains produced by targeted insertion of EYFP and ECFP into the ROSA26 locus. BMC Dev. Biol. *1*, 4.

Stolfi, A., Gainous, T.B., Young, J.J., Mori, A., Levine, M., and Christiaen, L. (2010). Early chordate origins of the vertebrate second heart field. Science *329*, 565–568.

Tajbakhsh, S., Rocancourt, D., and Buckingham, M. (1996). Muscle progenitor cells failing to respond to positional cues adopt non-myogenic fates in myf-5 null mice. Nature *384*, 266–270.

Tajbakhsh, S., Rocancourt, D., Cossu, G., and Buckingham, M. (1997). Redefining the genetic hierarchies controlling skeletal myogenesis: *Pax-3* and *Myf-5* act upstream of *MyoD*. Cell *89*, 127–138.

Theis, S., Patel, K., Valasek, P., Otto, A., Pu, Q., Harel, I., Tzahor, E., Tajbakhsh, S., Christ, B., and Huang, R. (2010). The occipital lateral plate mesoderm is a novel source for vertebrate neck musculature. Development *137*, 2961–2971.

Tzahor, E., and Evans, S.M. (2011). Pharyngeal mesoderm development during embryogenesis: implications for both heart and head myogenesis. Cardiovasc. Res. *91*, 196–202.

Yazaki, E., and Sifrim, D. (2012). Anatomy and physiology of the esophageal body. Dis. Esophagus *25*, 292–298.

Yokomizo, T., Yamada-Inagawa, T., Yzaguirre, A.D., Chen, M.J., Speck, N.A., and Dzierzak, E. (2012). Whole-mount three-dimensional imaging of internally localized immunostained cells within mouse embryos. Nat. Protoc. *7*, 421–431.

Zhao, W., and Dhoot, G.K. (2000). Both smooth and skeletal muscle precursors are present in foetal mouse oesophagus and they follow different differentiation pathways. Dev. Dyn. *218*, 587–602.